UNCLASSIFIED

~~CONFIDENTIAL~~

Copy No.

RM No. L8J21

NACA RM No. L8J21

NACA

RESEARCH MEMORANDUM

THE EFFECT OF AIR JETS SIMULATING CHINES OR MULTIPLE STEPS ON THE HYDRODYNAMIC CHARACTERISTICS OF A STREAMLINE FUSELAGE

By

Bernard Weinflash

Langley Aeronautical Laboratory
Langley Field, Va.

NATIONAL ADVISORY COMMITTEE FOR AERONAUTICS

WASHINGTON

January 7, 1949

~~CONFIDENTIAL~~

UNCLASSIFIED

NATIONAL ADVISORY COMMITTEE FOR AERONAUTICS

RESEARCH MEMORANDUM

THE EFFECT OF AIR JETS SIMULATING CHINES OR MULTIPLE STEPS ON THE HYDRODYNAMIC CHARACTERISTICS OF A STREAMLINE FUSELAGE

By Bernard Weinflash

SUMMARY

Preliminary tests were made in order to determine the effect of forced ventilation on the hydrodynamic characteristics of a $\frac{1}{12}$-size model of a streamline fuselage of a hypothetical transonic airplane. This forced ventilation consisted of air ejected at about 300 feet per second through small orifices distributed over the fuselage bottom in a series of patterns simulating chines or multiple steps.

Free-to-trim tests were made at speeds up to 60 feet per second with the load on the water varied with speed. Data are presented on the resistance, trim, and effective hydrodynamic lift for the basic model and for each of the jet configurations.

Without jets the resistance of the basic model was very large. All of the jet configurations resulted in improvements in the hydrodynamic performance of the model, especially at the higher speeds. The chine configurations generally gave better results than the multiple step configurations.

The best results were obtained with the jet configurations simulating 45° chines, 60° chines, and multiple forward V-steps. At one-half the assumed take-off speed, the 45° chines reduced the resistance of the streamline body from 15.7 pounds to 3.7 pounds and increased the effective hydrodynamic lift from 0.9 pound to 4.3 pounds.

The amount of air required to effect the improvements in the hydrodynamic characteristics of the streamline body was approximately $7\frac{1}{2}$ percent of the air flow through the compressor of the hypothetical airplane.

INTRODUCTION

In order to achieve minimum aerodynamic drag most airplanes designed to fly at transonic speeds are constructed with fuselages having circular or oval cross sections. Unfortunately, such sections in a seaplane hull make it inefficient from the standpoint of hydrodynamic performance. When a hull having a circular or oval cross section moves along a water surface at high speeds, the water flowing up around the convex bottom and sides of the hull creates a suction force which keeps the hull low in the water and thus causes a large hydrodynamic resistance which increases rapidly with speed. The existence of such a suction force has already been demonstrated by a number of earlier investigators (references 1 and 2).

One method of providing a means by which streamline bodies can be used for water-based airplanes is given in reference 3. Another possibility is the suggestion of Mr. Grover C. Loening, made at the 1946 meeting of the NACA subcommittee on seaplanes, that forced ventilation through small orifices, distributed over the fuselage bottom in patterns simulating steps or chines, might sufficiently reduce the suction forces to bring the hydrodynamic resistance of such a streamline body down to a reasonable figure. He also suggested that enough air for this purpose might be obtained by temporarily diverting a small percentage of the air passing through the turbojet compressors. In order to determine the feasibility of Mr. Loening's idea, a preliminary investigation has been made of the effect of several simple jet configurations, simulating steps or chines, on the hydrodynamic resistance, lift, and trim of a model of a typical high-speed fuselage.

DESCRIPTION OF MODEL

The model, designated Langley tank model 229A, was a $\frac{1}{12}$-size model of the fuselage of the hypothetical high-speed airplane described in reference 4. The principal dimensions and characteristics of the model are given in figure 1. For convenience of reference, distances from the nose measured along the center line are designated as stations. Offsets of the fuselage are given in table I. The model had a fineness ratio of 8.44, a volume of 585 cubic inches, and weighed about 15.7 pounds.

An open brass box was inserted into the top of the model to keep the model airtight and yet allow it to trim about its low center of gravity. Two hundred and sixty-four stainless-steel tubes (0.026 inch inside diameter) were inserted into the bottom of the model approximately normal to the surface at locations shown in figure 2. The outer ends of all the tubes were flush with the outer surface of the model and, except when being used in a particular jet configuration, were kept plugged. Representative chine and multiple-step configurations are shown in figure 3. All the jet patterns tested are listed in table II.

APPARATUS AND TEST PROCEDURE

The tests were conducted in Langley tank no. 2. The model was arranged on the staff of the towing gear as shown in figure 4. The model was supported at the center of gravity and towed free to rise and free to trim up to about 20°. A dashpot was used to damp out oscillations in trim.

In all of the simple chine or multiple-step configurations, JC 1 to JC 8, the flow of air used was about 0.008 pound per second with a jet velocity of about 300 feet per second. For the configuration JC 9 which was a combination of 45° chines and forward V-steps, the air flow was 0.016 pound per second. The configuration with all jets opened, JC 10, was tested with air flows of both 0.008 and 0.016 pound per second. Air was supplied to the model from a high-pressure air bottle equipped with a regulator, and a calibrated venturi tube was used to measure the air flow.

The load on the water was varied with speed assuming a constant aerodynamic lift coefficient for the hypothetical airplane. For each jet configuration measurements were taken of resistance, trim, and rise at constant speeds up to 60 feet per second except where the trend of the data indicated that further measurements would prove of little value.

Only approximate values of resistance were determined in the speed range between 60 feet per second and the assumed take-off speed of 70 feet per second, because at these speeds practically all of the model was out of the water and slight variations in wetted surface caused the readings to become quite erratic. The approximate values for each of the better configurations, however, were definitely less than the maximum resistance measured below 60 feet per second.

RESULTS AND DISCUSSION

The results obtained with the various jet configurations as well as comparisons of these results are given in figures 5 to 17. A description of each of these configurations is given in table II.

Resistance

The resistance of the basic model (fig. 5) rose rapidly with speed, increasing to 19.5 pounds at 40 feet per second with no indication of any reduction in the rate of increase. Measurements at higher speeds with the basic model were considered unwarranted in view of the alterations in the testing gear that would have been required.

As shown in figure 10, the resistances for all of the various chine configurations were about the same as that for the basic model up to about 15 feet per second. Above this speed, the resistance obtained with each configuration was reduced as the simulated chines were placed at greater angles from the keel line, and reached a minimum at the 45° location for which the resistance did not exceed 4.6 pounds. When the jet chines were moved to 60°, the resistance was generally somewhat higher reaching a maximum of 4.9 pounds for the take-off speed range.

The resistances for the three multiple-step configurations were also the same as for the basic model up to about 15 feet per second (fig. 14). Above this speed, the lowest resistance was obtained with the forward V-steps. The aft V-steps configuration appeared to be slightly better than the straight-across steps. The maximum resistance with the forward V-steps was 4.9 pounds; with the aft V-steps was 5.3 pounds; and with the straight-across steps was 5.9 pounds.

It is interesting to note the close similarity in results obtained with the 45° chine configuration and the best of the multiple-step configurations (fig. 15). Up to 40 feet per second, the resistance curves for these two quite dissimilar configurations were practically identical. Above 40 feet per second, the 45° chines were slightly better than the multiple forward V-steps.

When these two configurations were combined, the results obtained (fig. 16) were not better than those obtained by running them individually, even though twice as much air was used for the combination.

The results with all of the jets unplugged are shown in figure 17. When the air flow of 0.016 pound per second was used, the resistance at the intermediate speeds was appreciably lower than for the best of the simple configurations. At higher speeds, however, the resistance was not appreciably different from the results obtained with the better simple configurations. The over-all improvement was not enough to warrant the additional amount of air that would have to be used or the more complicated construction that would be required.

Since the slope of the resistance curve for the basic model is much steeper than that for any of the jet configurations, the reduction in resistance effected by the use of the jets increased rapidly with speed. At 35 feet per second, which was one-half the assumed take-off speed, the resistance of the model for most of the jet configurations was only about 25 percent of the resistance of the basic model.

Appreciable differences existed, however, among the results obtained with the simple jet configurations. For example, at 35 feet per second, the resistance of 3.7 pounds using 45° chines (fig. 8) was about 20 percent less than the resistance of 4.6 pounds using 30° chines (fig. 7). This represents a difference in resistance of 1550 pounds, full size. The best of the simple jet configurations were the 45° chines, the 60° chines, and the forward V-steps. In general, the chine configurations gave better results than the step configurations.

The maximum resistances for even the better jet configurations occurred at the upper end of the speed range, near take-off speed, where the load on the water was very small. This result is quite different from the results obtained with conventional flying-boat hulls where the resistance reaches a maximum in the lower part of the speed range and then decreases as the speed is increased to take-off. This failure of the resistance to decrease with increasing speed in the planing range could probably be overcome by further research.

Effective Hydrodynamic Lift

Effective hydrodynamic lift L is defined as the difference between the total lift at a given speed and the hydrostatic lift of the model at the same trim and rise. This lift was calculated for each speed by subtracting from the load on the water the static buoyancy corresponding to the immersed volume of the model at the trim and rise measured at that speed.

Effective hydrodynamic lift was plotted rather than the more conventional rise because it was believed to be more informative as to the results obtained. For example, a comparison between the load on the water Δ and the effective hydrodynamic lift demonstrates the efficiency of the jets in reducing the suction forces. Then, too, for this particular type of hull the hydrostatic lift remains an appreciable part of the total up to much higher speeds than is the case for the conventional flying boat or seaplane. Thus, the ratio of effective hydrodynamic lift to resistance L/R is a more fundamental measure of planing efficiency than the ratio of load on the water to resistance Δ/R. The ratio L/R permits a direct comparison between the desirable vertical component and the undesirable horizontal component of the hydrodynamic forces acting on the hull.

At speeds up to about 15 feet per second, the vertical component of the planing force was insufficient to overcome the vertical component of the hydrodynamic suction forces and L was therefore negative with or without jets. The variations in the shapes of the lift curves in this low-speed range were partly due to differences in wave patterns around the hull. At higher speeds, the shapes of the lift curves for the different jet configurations became more uniform.

With increasing speed, the suction forces on the basic model grew larger almost as rapidly as the lifting forces, the effective hydrodynamic lift reaching a maximum of only 1 pound. In contrast to this, the use of any of the jet configurations diverted the transverse flow of water up around the sides of the model and thus greatly reduced the suction forces. The effective hydrodynamic lift increased rapidly with speed, and, for most of the jet configurations, reached a maximum value of about 4 pounds at 35 feet per second. At this speed, the use of the 45° jet chines increased the effective hydrodynamic lift from 0.9 pound to 4.3 pounds. Above this speed, the lift curve gradually approached the curve for load on the water which is, of course, the upper limit of the lift curve.

The effective hydrodynamic lift for most of the jet patterns did not vary as much as the resistance at speeds above 15 feet per second. Evidently, while most of the jet configurations produced about the same effective hydrodynamic lift at a given speed, the differences in trim and wetted areas for the various patterns were sufficient to cause quite appreciable changes in resistance. As a result, each jet configuration caused the streamline body to simulate a planing surface of a different degree of efficiency, L/R.

A comparison between the curves of L/R and the curves of Δ/R of the basic model and the 45° chine configuration is made in figure 18. Up to about 15 feet per second, the curves of Δ/R were identical with and without jets, but the curve of L/R for the 45° jet configuration was definitely higher than that for the basic model. This shows that at these lower speeds, the use of jets had already increased the planing lift, but had not yet affected the resistance. At higher speeds, the jets affected the resistance as well as the dynamic lift and both the curves of L/R and the curves of Δ/R showed definite improvement of the jet configuration over the basic model.

The efficiency for even the best of the jet patterns as defined by either L/R or Δ/R was still quite low. For example, the ratio L/R for the 45° chine configuration was about 1.1 at 35 feet per second and the ratio Δ/R at this speed was about 1.5. This is appreciably lower than the ratio Δ/R of about 5.0 for a conventional, $22\frac{1}{2}^{\circ}$ dead-rise planing surface at its best trim. It should be remembered, however, that the 45° chine configuration would probably give better results if it were also run at its best trim. Further increase in efficiency might be obtained by changes in jet spacing, jet size, or fineness ratio of fuselage.

Trim

The reduction in suction forces caused by the use of air jets is further shown when the trim tracks of any of the jet configurations are compared with those of the basic model.

With no jets (fig. 5), the model trimmed up sharply from 5° at 15 feet per second to 18.6° at 17 feet per second and remained against the trim stops (set at about 20°) from 25 feet per second on.

The trim track for the 15° chine configuration (fig. 6) rose to a peak of 12.3° at 22 feet per second and dropped to 10.3° at 40 feet per second. The trim track for the 60° chine configuration (fig. 9) did not peak at all, but rose rather rapidly to 7.6° at 17 feet per second and then gradually increased to 10.8° at 60 feet per second. The trim tracks of the other jet configurations were all quite similar (figs. 10 and 14), rising to a peak of about 9° at approximately 20 feet per second and then decreasing to about 7° at speeds above 25 feet per second.

From visual observation (figs. 19 and 20), the center of pressure of the planing forces for the jet configurations was aft of the center of gravity for about the upper half of the speed range. Since the model was supported free to trim at the center of gravity, a purely planing hydrodynamic lift force would have exerted a bow-down moment and caused the model to trim much lower than it did. Evidently, none of the jet configurations were successful in eliminating all the suction forces and some suction force remained to act on the stern of the model and give it a bow-up moment.

Spray

The photographs in figure 19 give a visual comparison between the basic model and the various jet configurations at 35 feet per second. When no jets were used, the model ploughed through the water with the after half completely sucked under, a large amount of spray was projected forward, and a large sheet of spray was thrown out to either side. The spray patterns for the jet configurations showed appreciable improvement when compared with the basic model. Most of the model planed along the surface of the water with no forward spray and the water streamed cleanly back from the forward water line with little side spray.

The photographs in figure 20 show the variation in spray pattern with speed for both the basic model and the 45° chine configuration. At any given speed, the amount of spray with jets was much less than without jets, the improvement increasing with speed. An enlargement of one of these photographs is shown in figure 21 to bring out the outlines of one or two individual jets interacting with the water film.

Air Flow

The air flow of 0.008 pound per second used in the simple chine or jet configurations (JC 1 to 8) was arbitrarily selected and is not necessarily the minimum amount of air that could have been used. Although the effect of varying the air flow of a particular jet configuration was not included in the scope of this preliminary investigation, the results obtained with the two rates of air flow used when all jets were open (fig. 17) indicated that there was some variation in hydrodynamic performance with changes in air flow.

Operating the model with all jets open also proved to be appreciably less effective than most of the simple jet configurations when the same air flow of 0.008 pound per second was used. When twice this air flow was used with all jets open, the results obtained were practically the same as for the 45° chine configuration using an air flow of 0.008 pound per second.

The results obtained with the combination of the forward V-steps and 45° chines were no better than the results obtained by using either of these two configurations separately even though twice as much air was used for the combination. Evidently proper jet distribution is important in securing optimum results.

The air flow of 0.008 pound per second used in this preliminary investigation was equivalent to 4 pounds per second full size. The air flow through the compressors of the 3000-pound-thrust turbojet of the hypothetical airplane would be about 55 pounds per second at take-off speeds. Thus, the air flow of 0.008 pound per second would be about $7\frac{1}{2}$ percent of the air passing through the intakes of the hypothetical airplane. This method of scaling up the effect of the air flow assumes that all forces vary in the same way as the gravitational forces, and it is possible that viscous and surface tension forces may be of sufficient importance to give an appreciable scale effect.

CONCLUSIONS

The results of this preliminary investigation of the effect of high-velocity air jets simulating chines or multiple steps on the hydrodynamic performance of a streamline fuselage lead to the following conclusions. Although these conclusions are based solely on the results obtained with a single model, they are believed to be applicable to all streamline bodies.

1. The very high hydrodynamic resistance of the streamline body was greatly reduced when air was ejected at high velocity through certain patterns of fine jets in the fuselage bottom.

2. The effective hydrodynamic lift of the streamline body was appreciably increased by means of these air jets.

3. The use of these air jets caused the model to plane along the surface of the water at reasonable trims instead of ploughing half submerged through the water at excessively high trims.

4. None of the jet configurations completely eliminated the suction forces. The residual suction forces acted on the stern of the model causing the model to trim up somewhat.

5. Proper jet distribution was important in securing optimum results with a given air flow even though any of the jet configurations resulted in a great improvement in the poor hydrodynamic performance of the basic model.

6. The jet configurations simulating chines generally gave better results than those simulating multiple steps. The best of the simple jet configurations were the ones simulating chines at 45°, chines at 60°, and multiple forward V-steps.

7. The amount of air required to effect the improvement in the hydrodynamic performance of the streamline body was a small percentage of the air flow through the compressor of the hypothetical airplane.

Langley Aeronautical Laboratory
National Advisory Committee for Aeronautics
Langley Field, Va.

REFERENCES

1. Richardson, Holden C.: Aircraft Float Design. The Ronald Press Co., 1928, p. 18.

2. King, Douglas A.: Preliminary Tank Tests of an Outboard Float Having the Form of a Streamline Body of Revolution Fitted with a Hydrofoil. NACA ACR No. L4D06, 1944.

3. Dawson, John R., and Wadlin, Kenneth L.: Preliminary Tank Tests of NACA Hydro-Skis for High-Speed Airplanes. NACA RM No. L7I04, 1947.

4. King, Douglas A.: Tests of the Landing on Water of a Model of a High-Speed Airplane - Langley Tank Model 229. NACA RM No. L7I05, 1947.

TABLE I

OFFSETS FOR LANGLEY TANK MODEL 229A

[All dimensions are in inches.]

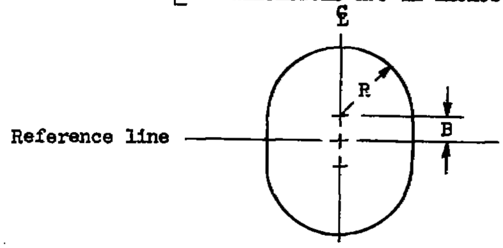

Distance from nose (station)	Distance from reference line to center of circle, B	Half-breadth or radius, R
0	0	0
.42	0	.16
.83	0	.33
1.25	0	.48
2.08	0	.77
4.17	0	1.39
6.25	0	1.88
8.33	0	2.20
10.42	0	2.39
12.50	0	2.48
14.58	0	2.50
20.83	0	2.50
21.67	0	2.50
22.92	0	2.49
25.00	0	2.45
27.08	0	2.37
29.17	.05	2.25
31.25	.13	2.08
33.33	.22	1.88
35.42	.34	1.65
37.50	.47	1.40
39.58	.60	1.14
42.22	.75	.83

NACA

TABLE II

JET CONFIGURATIONS INVESTIGATED

Jet configuration	Description	Figure
--------------------	Basic model — all jets plugged	5
JC 1	Simulated chines at 15°	6
JC 2	Simulated chines at 30°	7
JC 3	Simulated chines at 30° (based on center of curvature)	7
JC 4	Simulated chines at 45°	8
JC 5	Simulated chines at 60°	9
JC 1, JC 2, JC 4, JC 5	Comparison of various simulated chine configurations	10
JC 6	Simulated multiple steps — straight across	11
JC 7	Simulated multiple steps — forward V	12
JC 8	Simulated multiple steps — aft V	13
JC 6, JC 7, JC 8	Comparison of various simulated multiple step configurations	14
JC 4, JC 7	Comparison of 45° chines with multiple forward V-steps	15
JC 9	Combination of JC 4 and JC 7	16
JC 10	All jets open	17
--------------------	Comparison of Δ/R and L/R for simulated chines at 45°	18

NACA

[redacted]

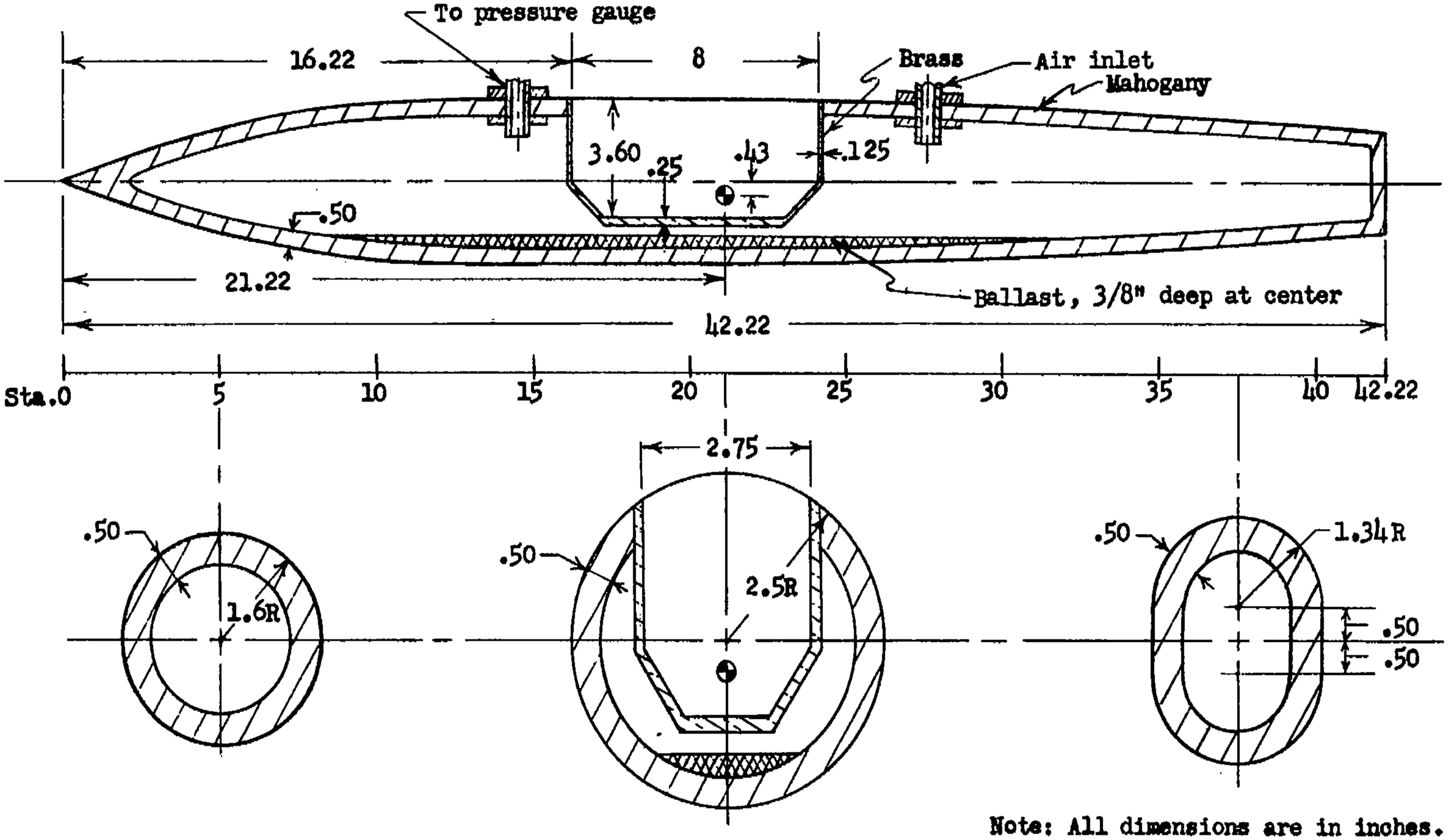

Figure 1.- Sketch of model 229A and typical sections.

[redacted]

[redacted]

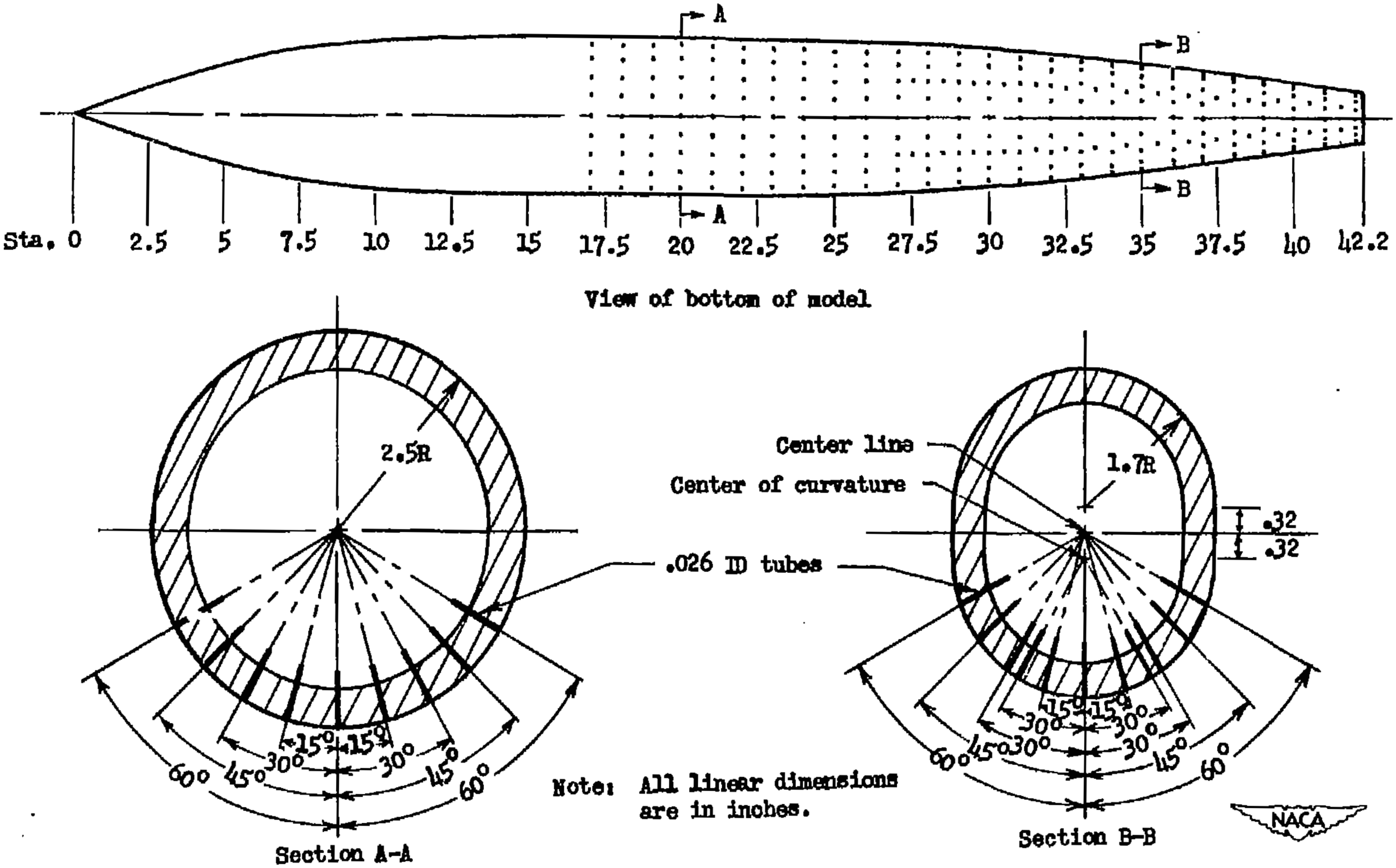

Figure 2.- Distribution of jets. (Model 229A.)

[redacted]

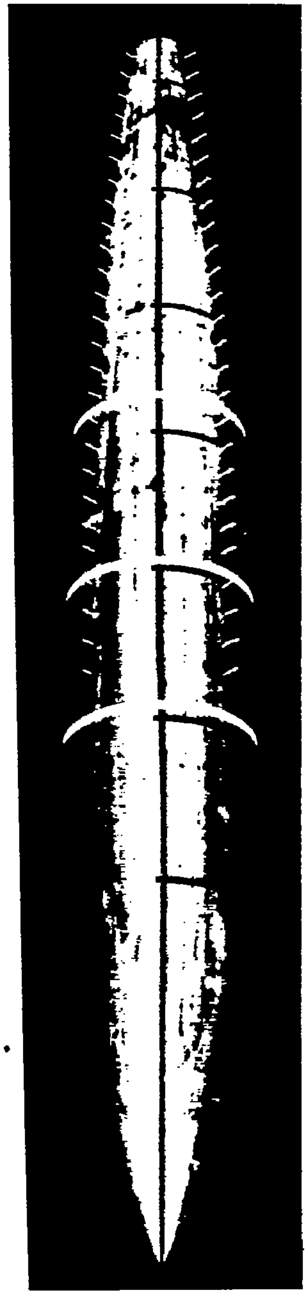

JC 4

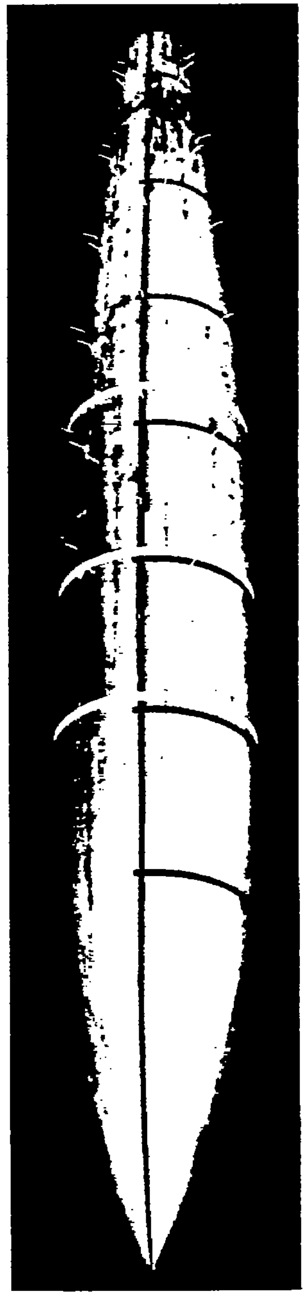

JC 7

Figure 3.- Bottom views of model showing typical jet configurations.
(Pins inserted to show location of jets.)

NACA
L-58315

[redacted]

[redacted]

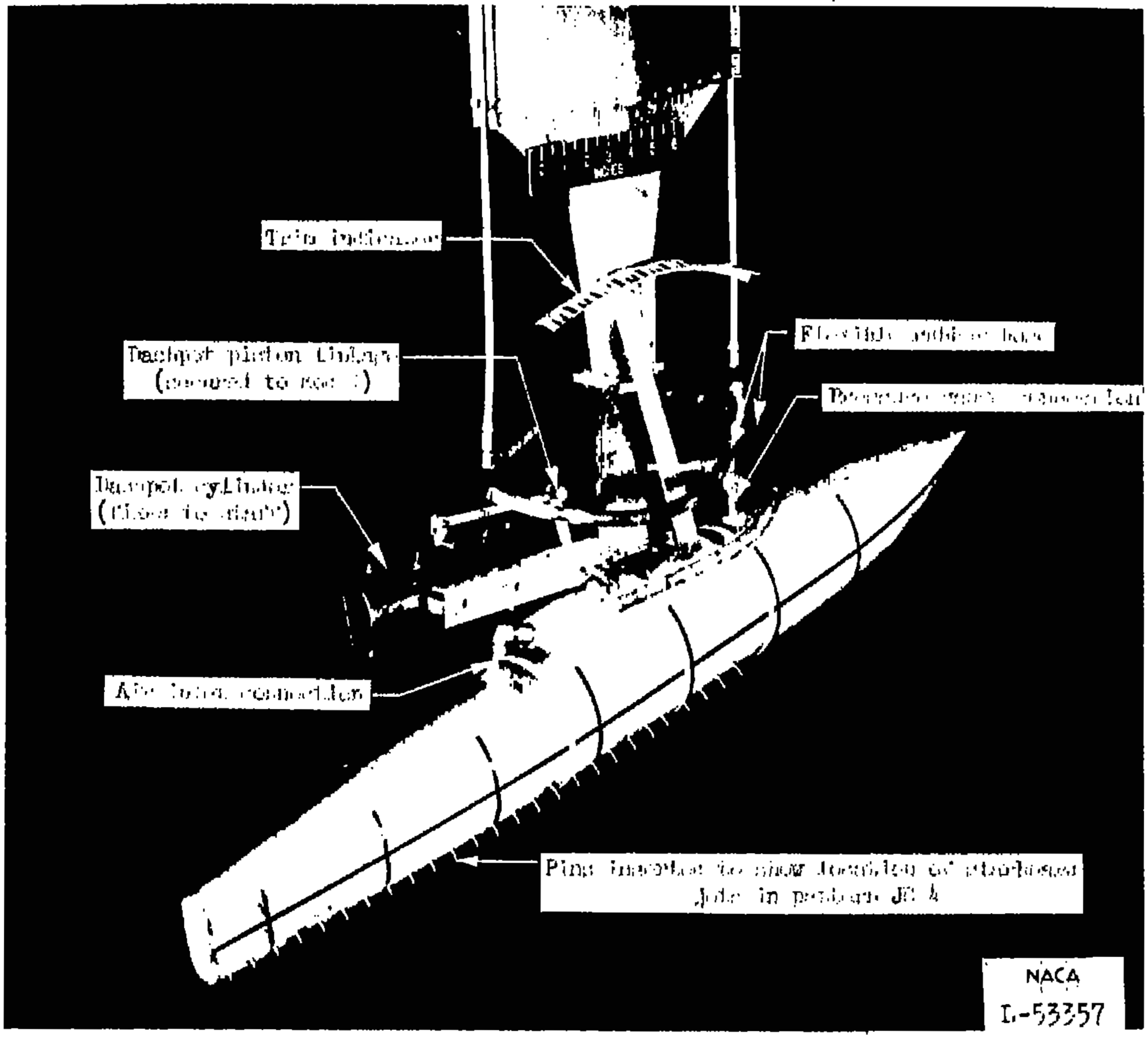

Figure 4.- Model 229A mounted for testing.

[redacted]

[redacted]

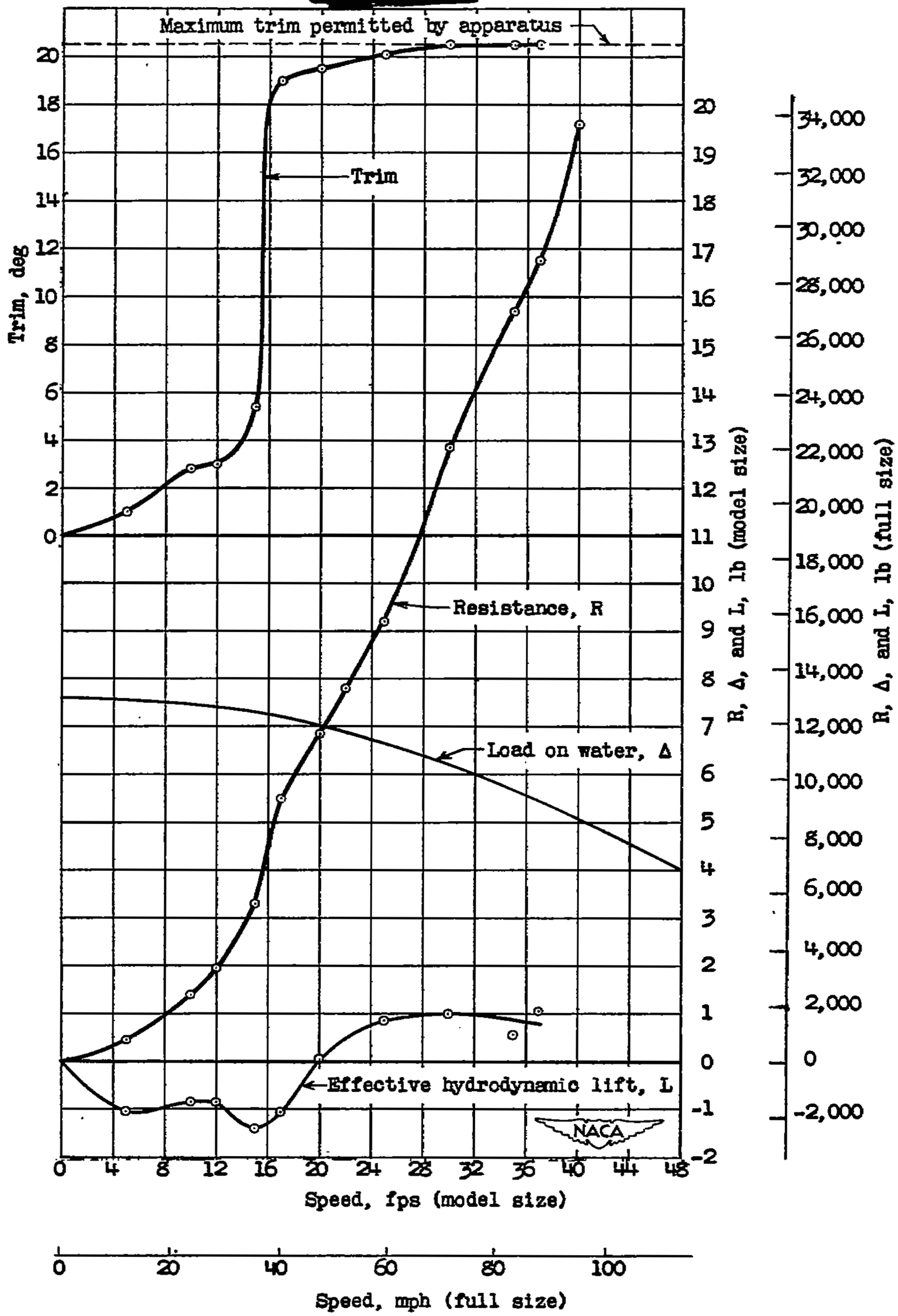

Figure 5.- Hydrodynamic characteristics of model 229A with no jets.

[redacted]

[redacted]

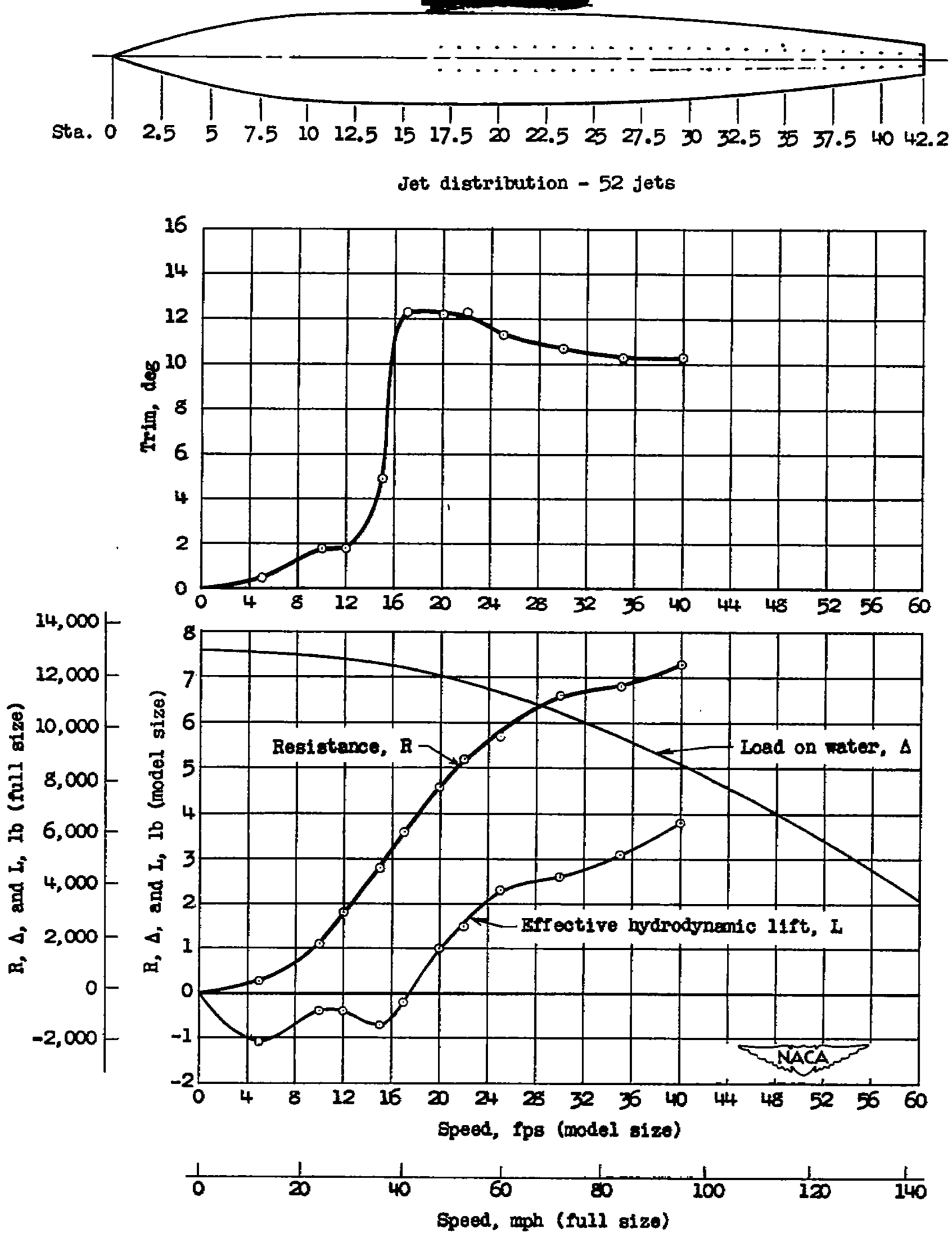

Figure 6.- Hydrodynamic characteristics of model 229A with simulated 15° chines (JC 1). Air flow = 0.008 pound per second, model size.

[redacted]

[redacted]

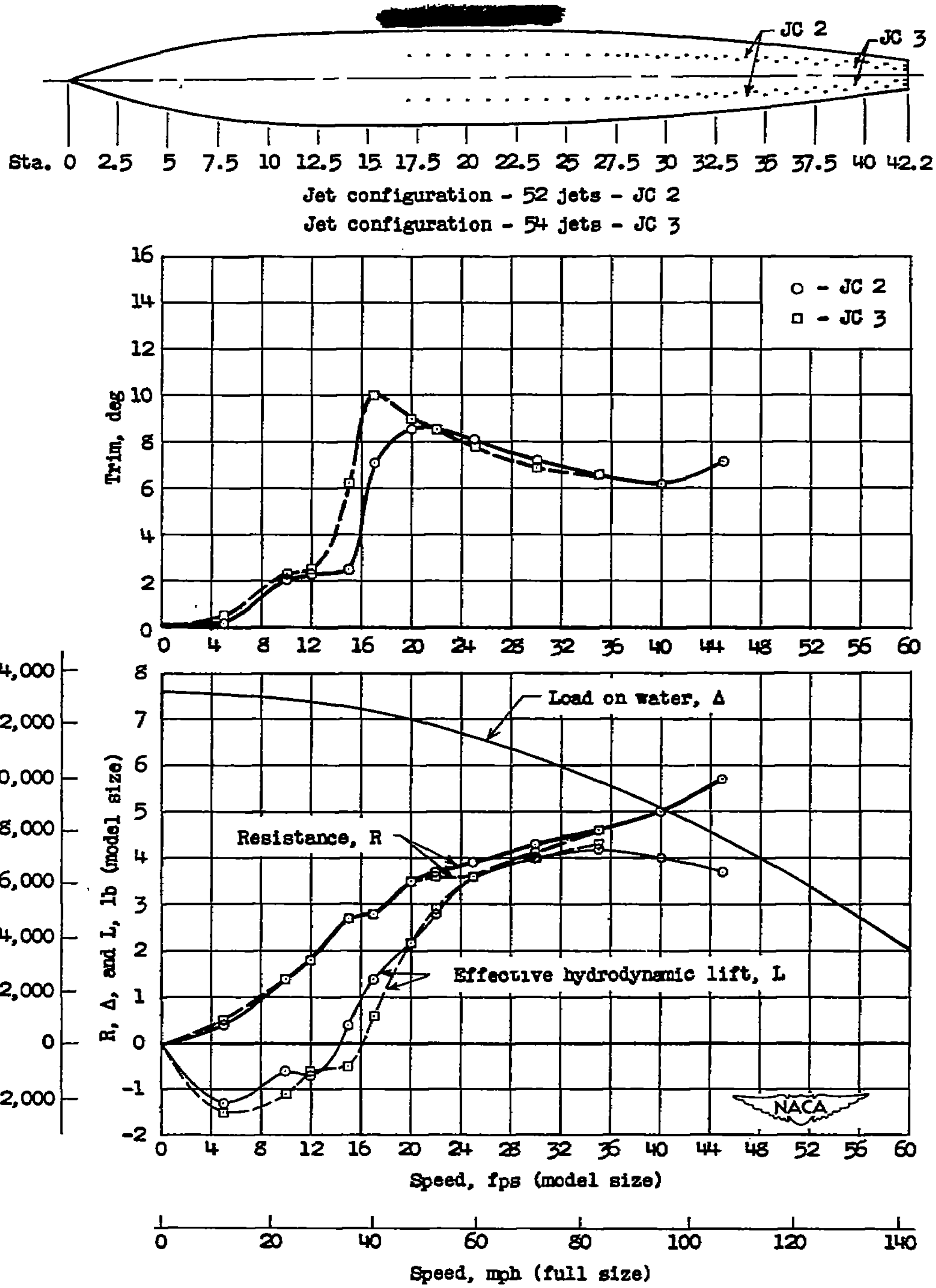

Figure 7.- Comparison of hydrodynamic characteristics of model 229A with simulated 30° chines based on center line (JC 2) and on center of curvature (JC 3). Air flow = 0.008 pound per second, model size.

[redacted]

[redacted]

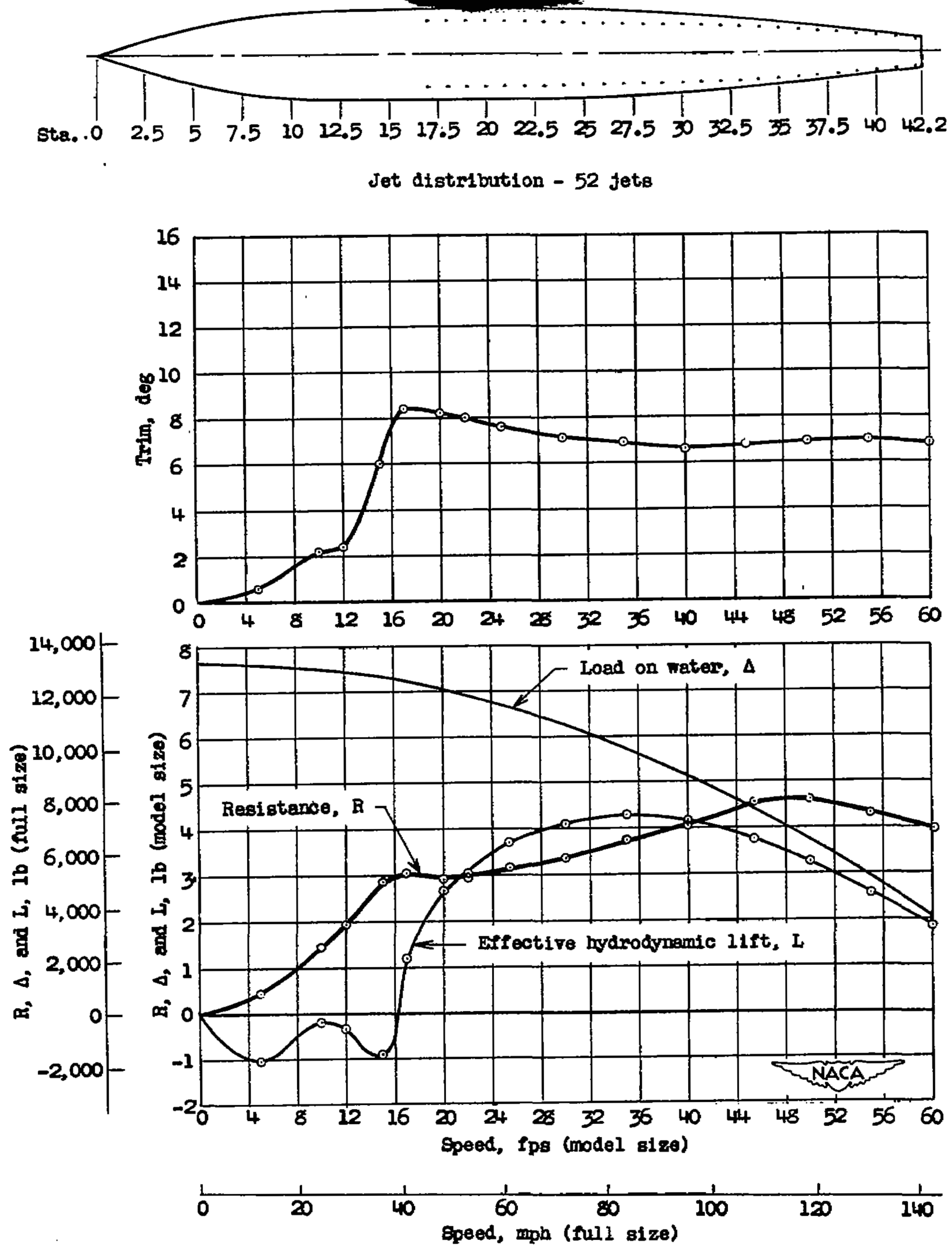

Figure 8.- Hydrodynamic characteristics of model 229A with simulated 45° chines (JC 4). Air flow = 0.008 pound per second, model size.

[redacted]

[redacted]

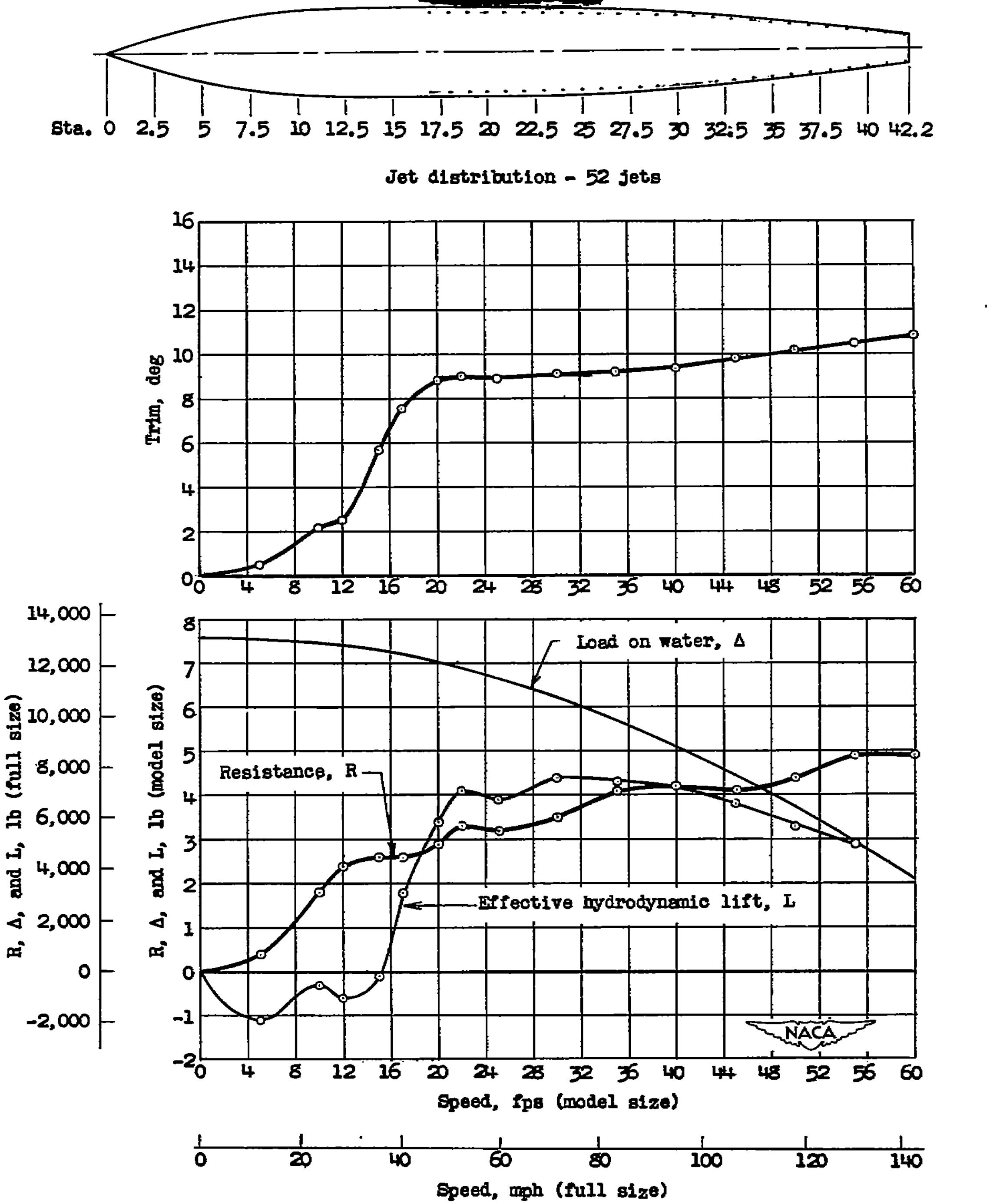

Figure 9.- Hydrodynamic characteristics of model 229A with simulated 60° chines (JC 5). Air flow = 0.008 pound per second, model size.

[redacted]

[redacted]

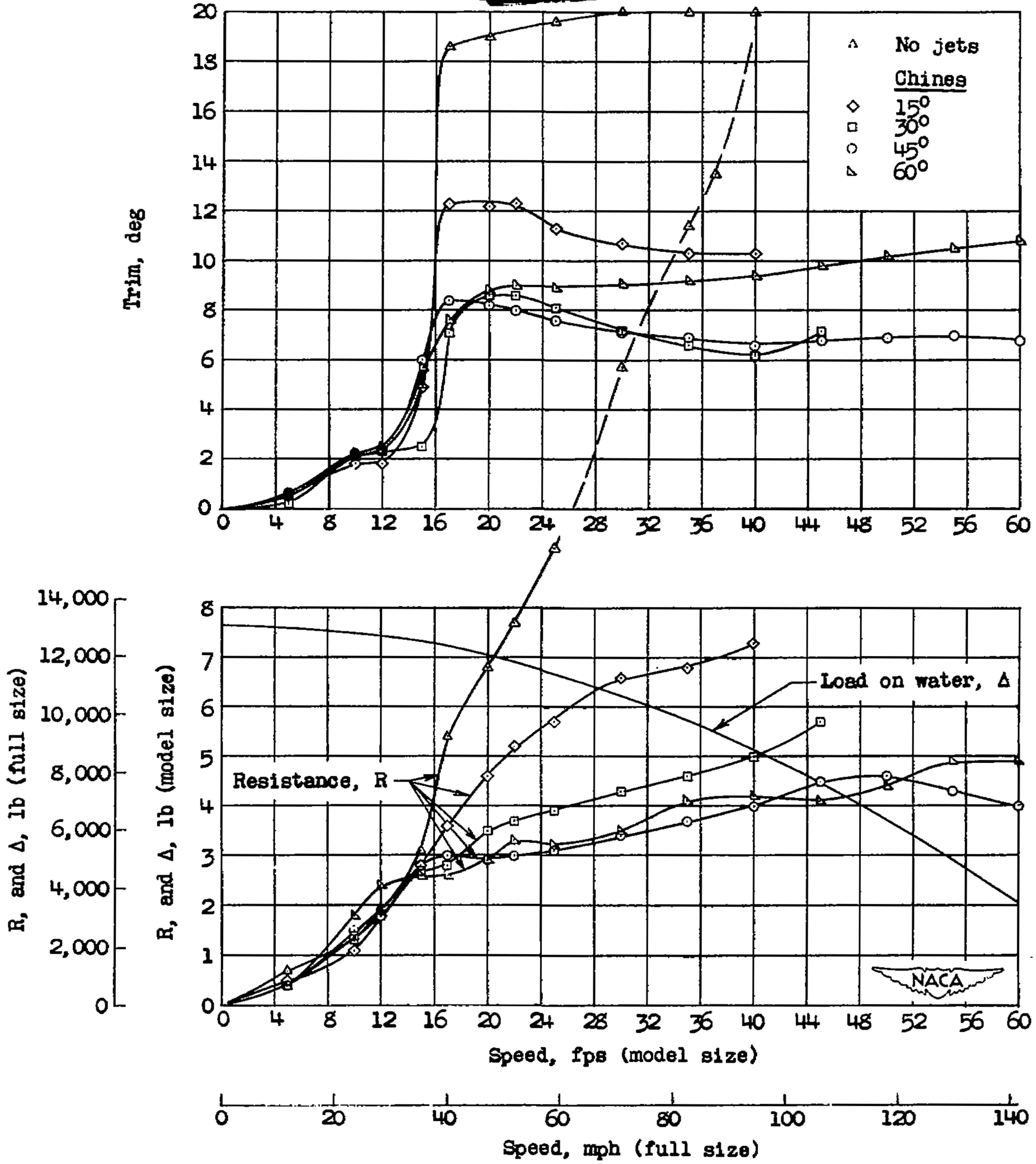

Figure 10.- Comparison of hydrodynamic characteristics of model 229A when modified by various simulated chine configurations. Air flow = 0.008 pound per second, model size.

[redacted]

[redacted]

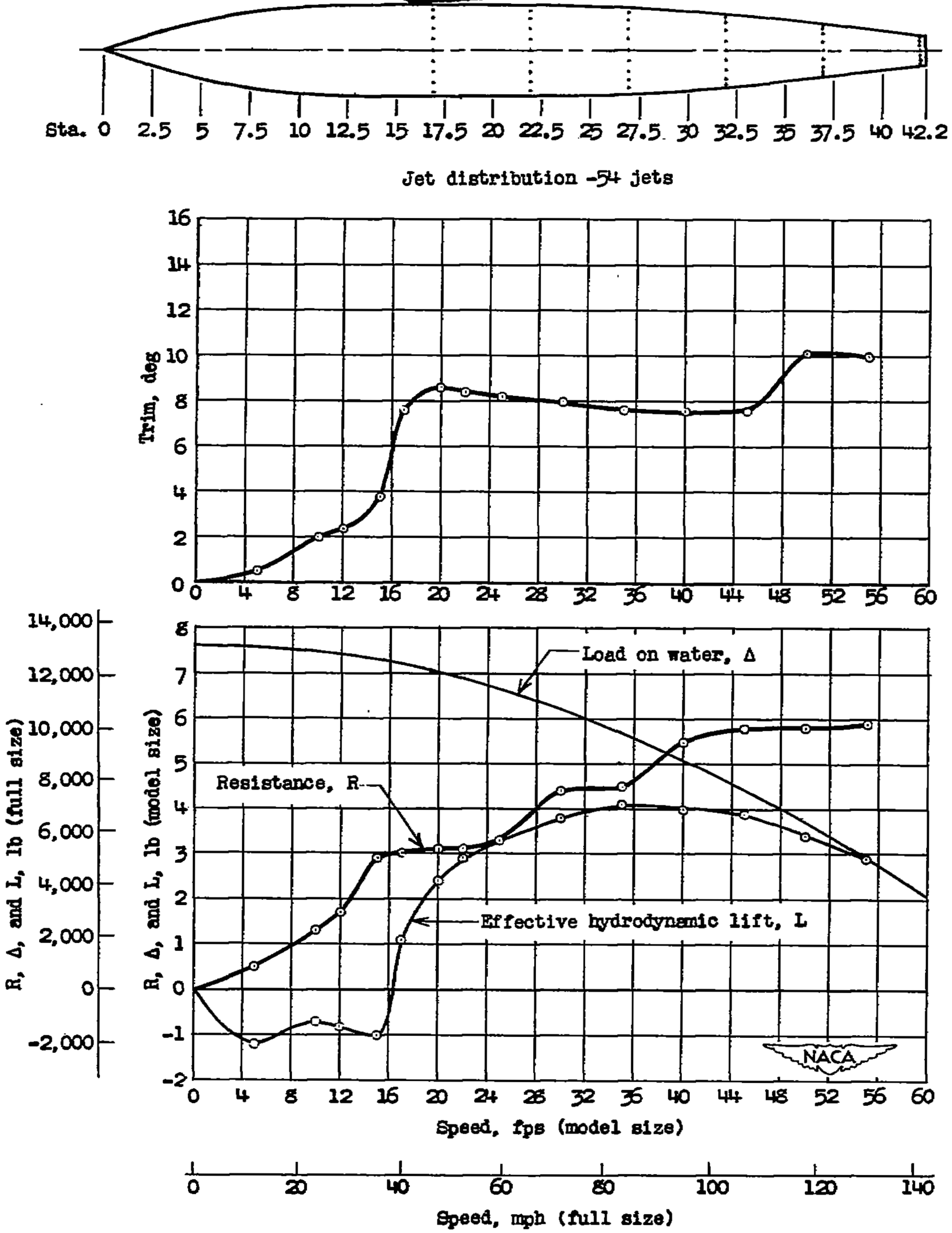

Figure 11.- Hydrodynamic characteristics of model 229A with simulated straight steps (JC 6). Air flow = 0.008 pound per second, model size. [redacted]

[redacted]

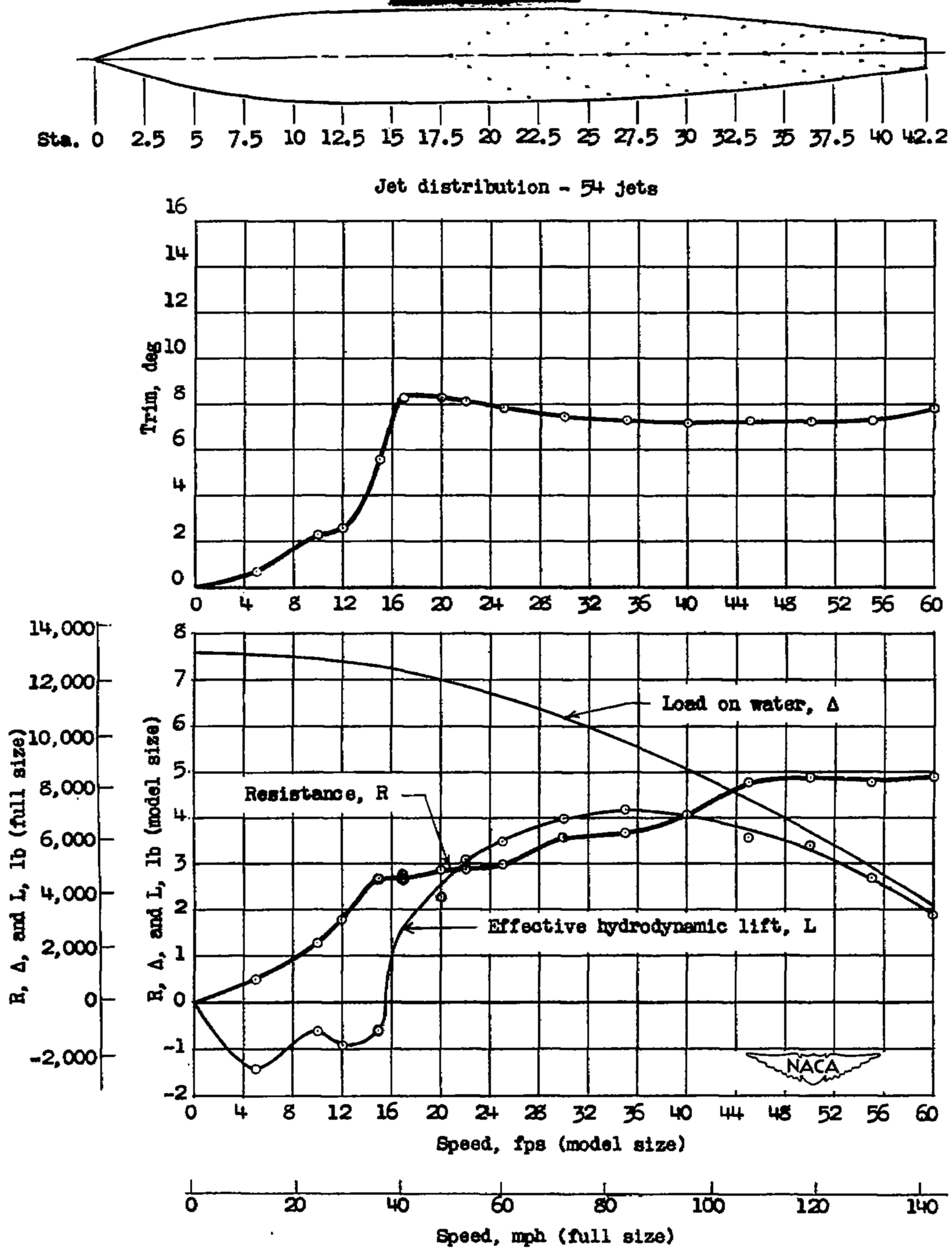

Figure 12.- Hydrodynamic characteristics of model 229A with simulated forward V-steps (JC 7). Air flow = 0.008 pound per second, model size.

[redacted]

[redacted]

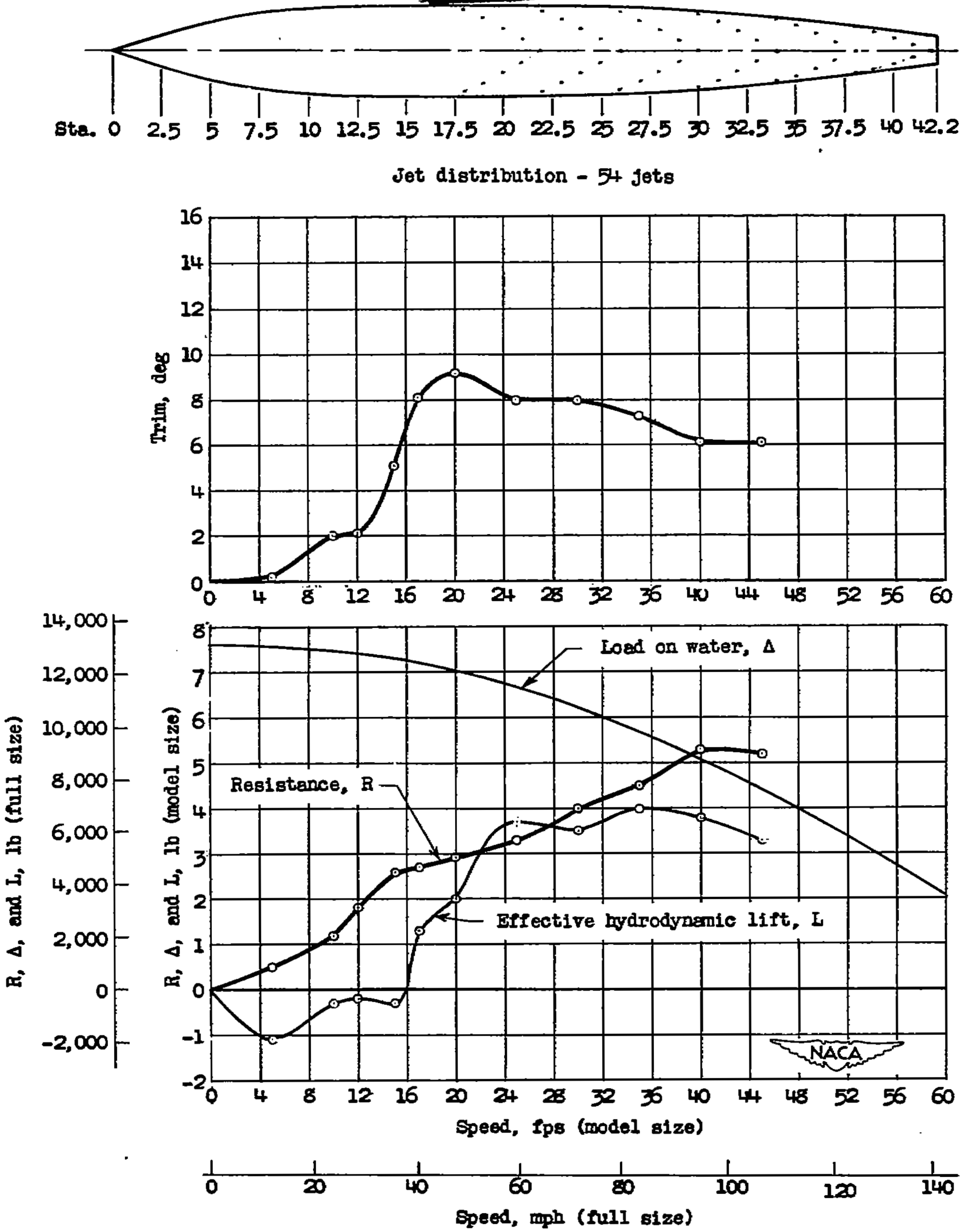

Figure 13.- Hydrodynamic characteristics of model 229A with simulated aft V-steps (JC 8). Air flow = 0.008 pound per second, model size.

[redacted]

[redacted]

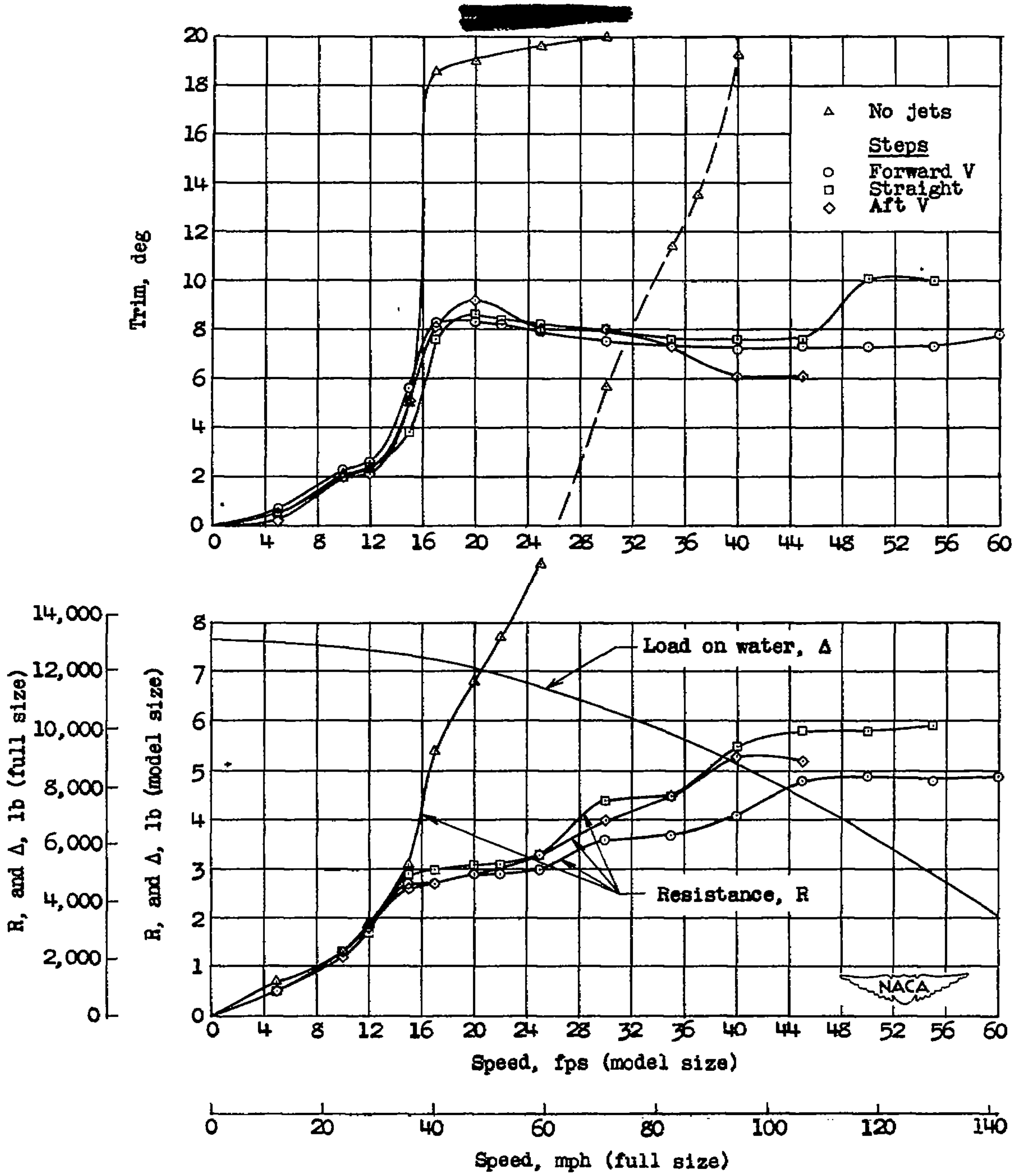

Figure 14.- Comparison of hydrodynamic characteristics of model 229A when modified by various simulated multiple step configurations. Air flow = 0.008 pound per second, model size.

[redacted]

[redacted]

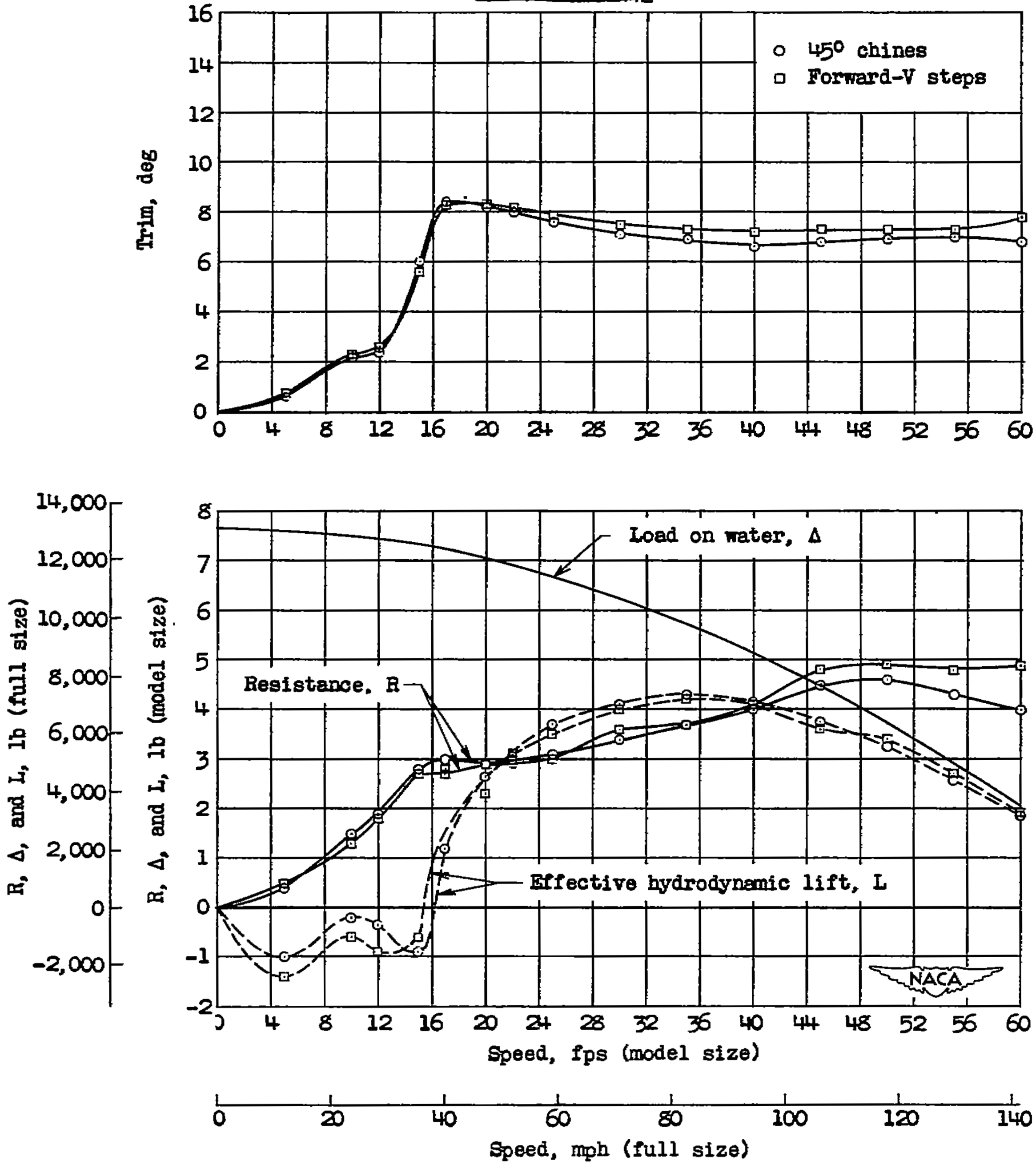

Figure 15.- Comparison of hydrodynamic characteristics of model 229A with simulated 45° chines and multiple forward V-steps. Air flow = 0.008 pound per second, model size.

[redacted]

[redacted]

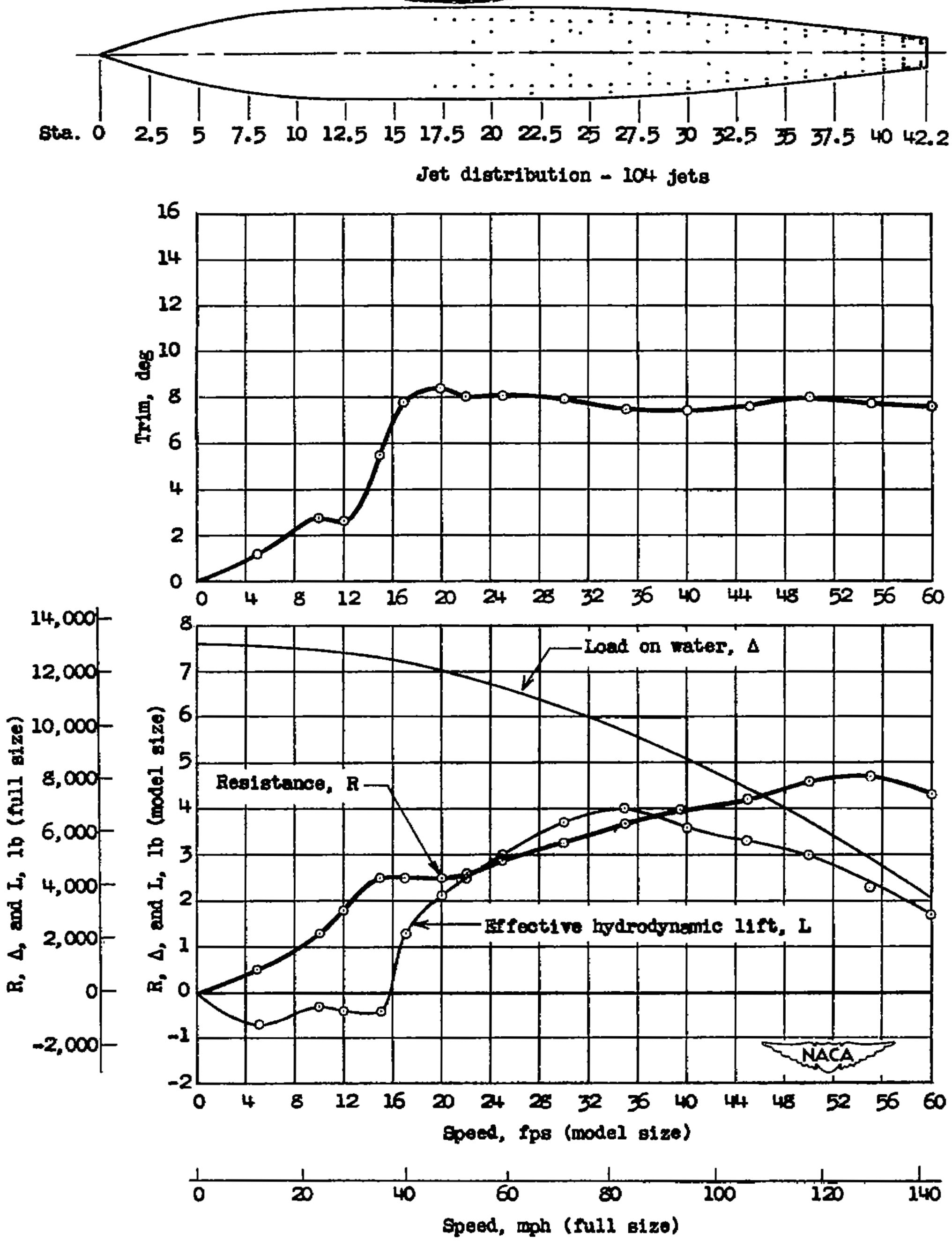

Figure 16.- Hydrodynamic characteristics of model 229A with simulated combination of forward V-steps and 45° chines (JC 9). Air flow = 0.016 pound per second, model size.

[redacted]

[redacted]

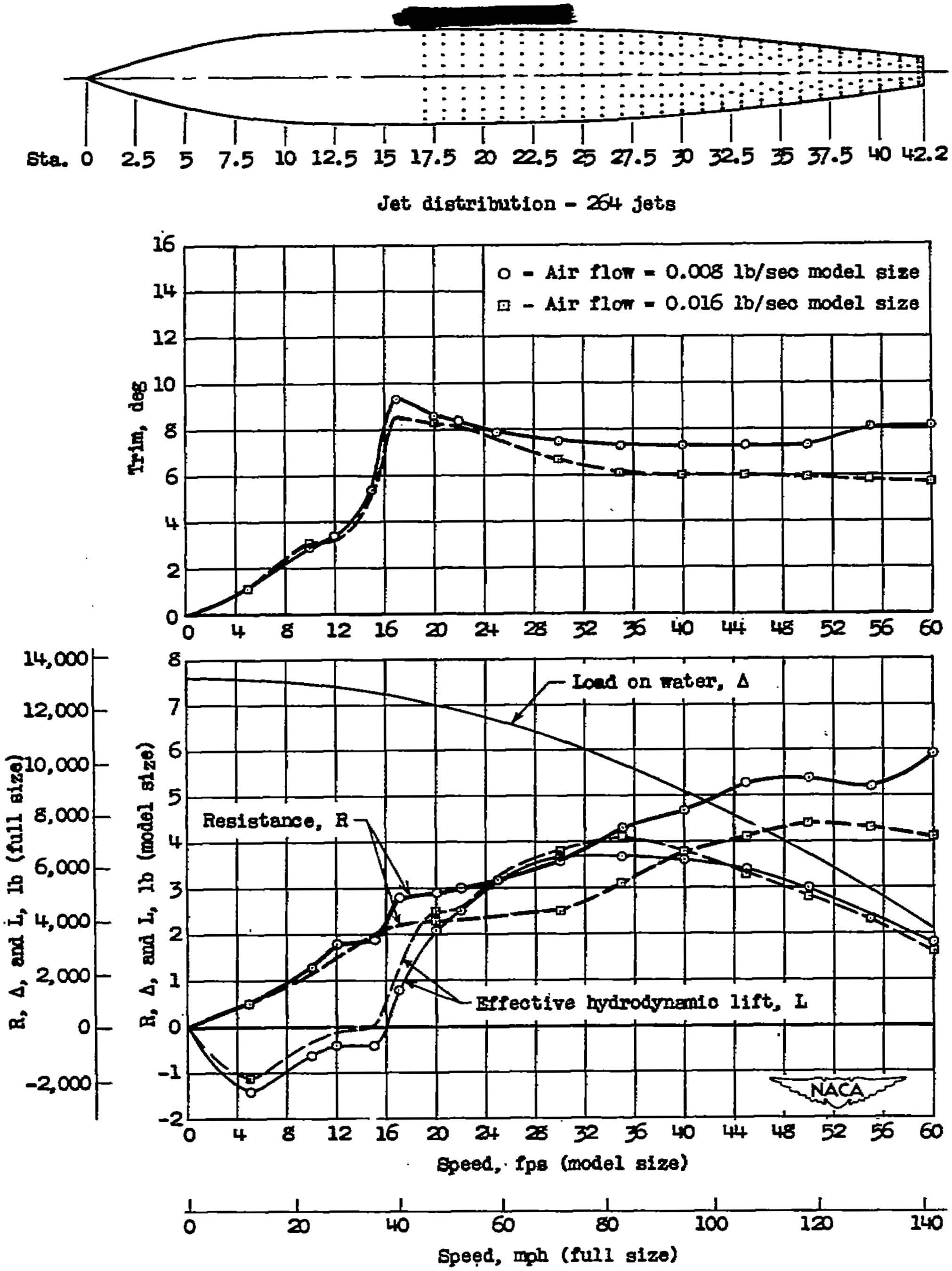

Figure 17.- Hydrodynamic characteristics of model 229A with all jets open (JC 10), comparing the effects of 0.008 pound per second and 0.016 pound per second air flow.

[redacted]

[redacted]

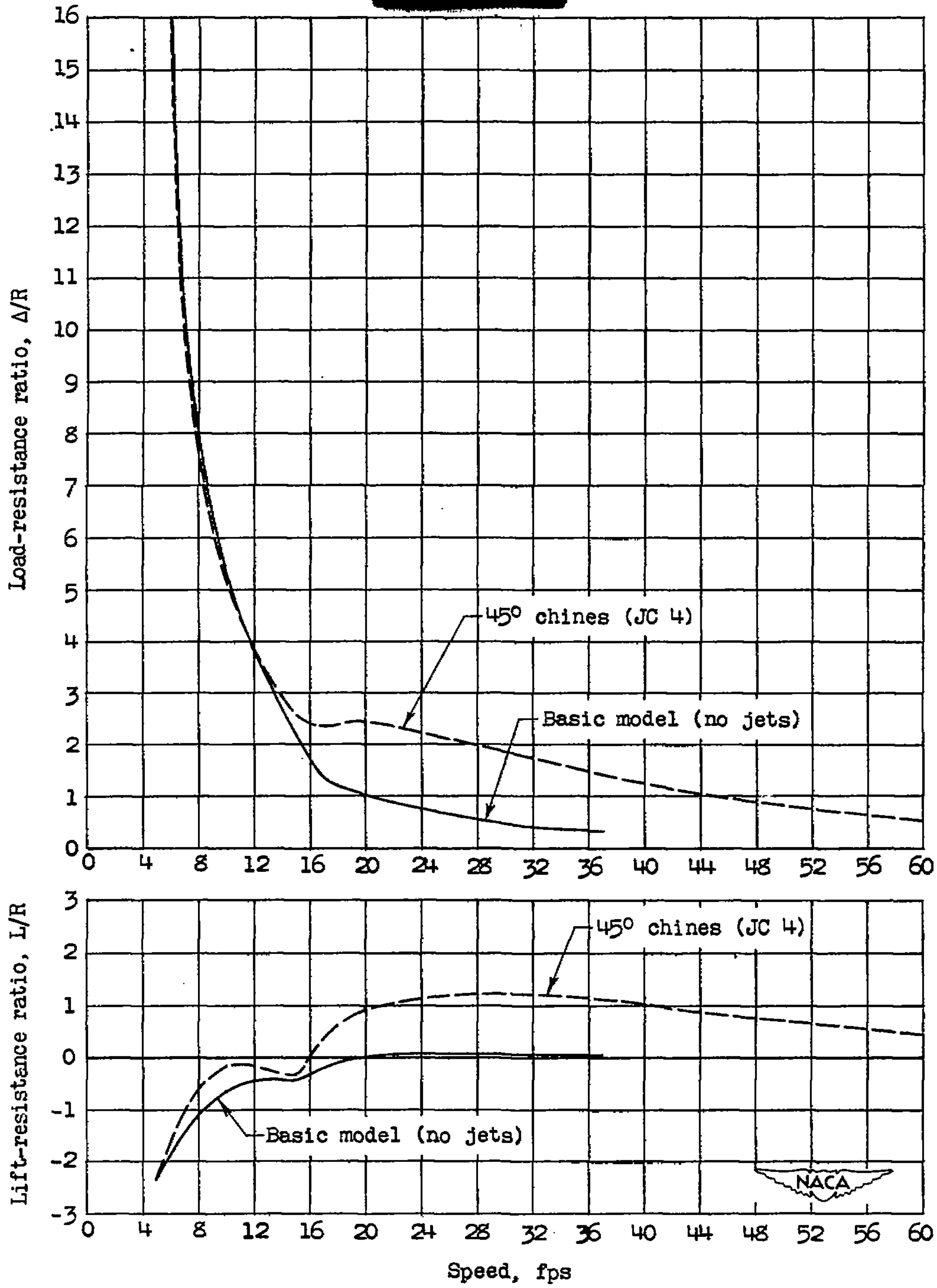

Figure 18.- Comparison of lift-resistance ratio and of load-resistance ratio between 45° chines jet configuration (JC 4) and the basic model with no jets. [redacted]

[redacted]

Basic model — no jets

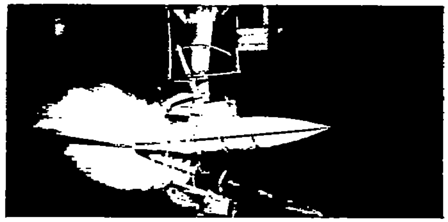

JC 6 — straight steps

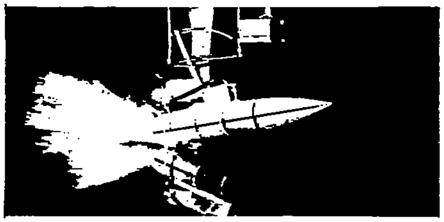

JC 1 — 15° chines

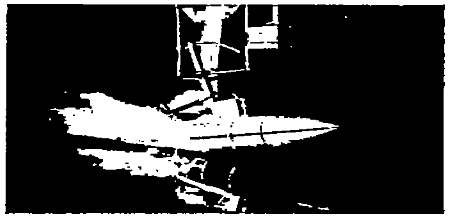

JC 7 — forward V-steps

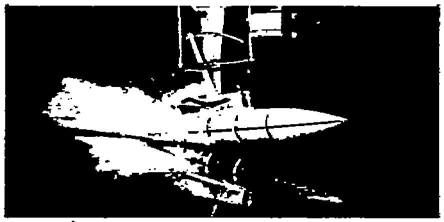

JC 2 — 30° chines

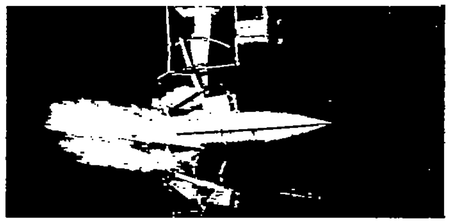

JC 8 — aft V-steps

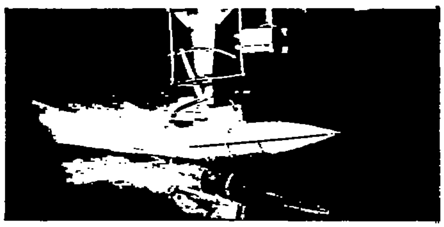

JC 4 — 45° chines

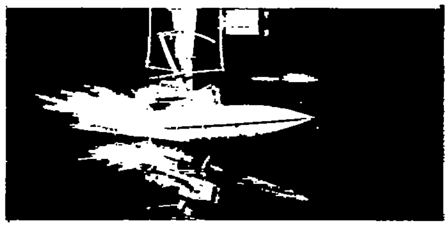

JC 9 — JC 4 plus JC 7

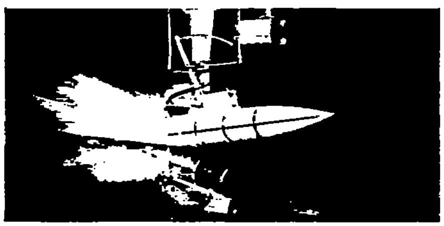

JC 5 — 60° chines

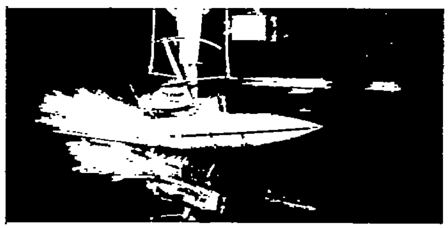

JC 10 — all jets open

Figure 19.- Comparison of spray characteristics at 35 feet per second.

[redacted]

NACA

[redacted]

10 fps

20 fps

35 fps

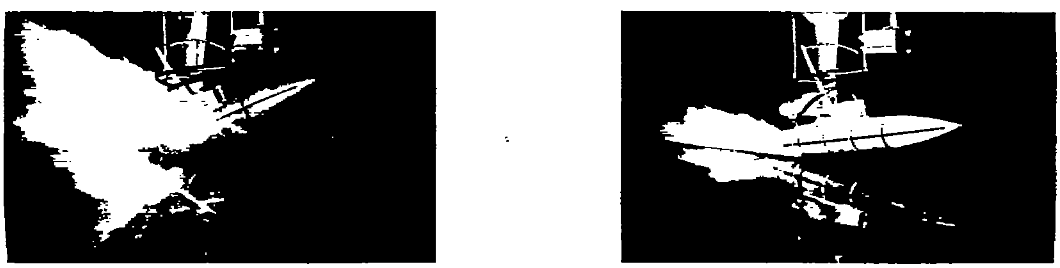

Basic model 50 fps 45° chines

Figure 20.- Comparison of 45° chines (JC 4) with basic model (no jets).

[redacted]

[redacted]

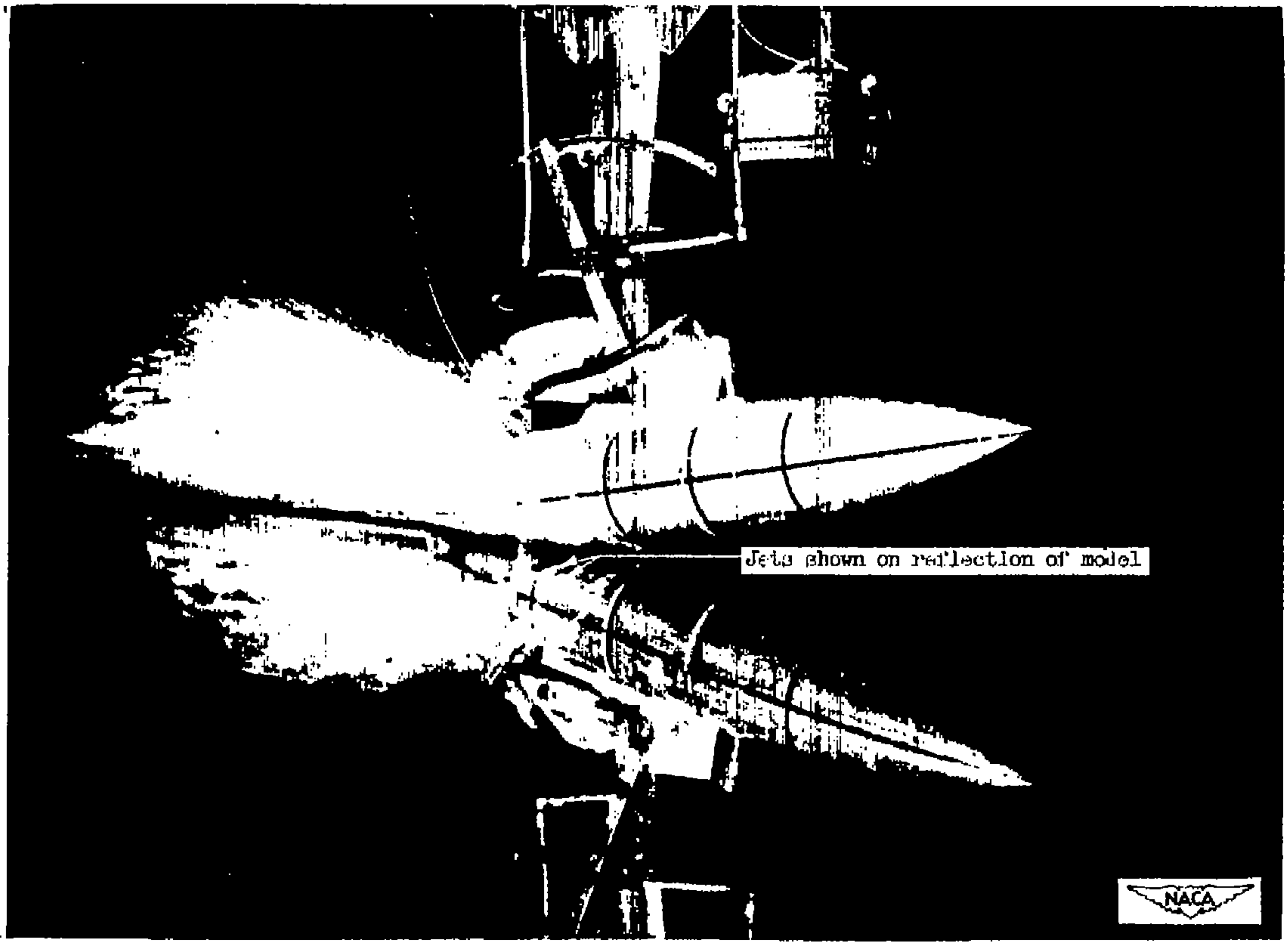

Figure 21.- Enlargement of photograph of 45° jet configuration (JC 4) to show individual jets interacting with film of water traveling up the side of the hull.

[redacted]